

Stephen J. Price
Alonso Peña
Neil G. Burnet
Raj Jena
Hadrian A. L. Green
T. Adrian Carpenter
John D. Pickard
Jonathan H. Gillard

Tissue signature characterisation of diffusion tensor abnormalities in cerebral gliomas

Received: 20 March 2004
Revised: 5 April 2004
Accepted: 8 April 2004
Published online: 25 June 2004
© Springer-Verlag 2004

S. J. Price · A. Peña · J. H. Gillard
Department of Radiology,
Addenbrooke's Hospital,
University of Cambridge,
Cambridge, CB2 2QQ, UK

S. J. Price · H. A. L. Green
T. A. Carpenter · J. D. Pickard
J. H. Gillard
Wolfson Brain Imaging Centre,
Addenbrooke's Hospital,
University of Cambridge,
Cambridge, CB2 2QQ, UK

S. J. Price (✉) · A. Peña · J. D. Pickard
Academic Neurosurgery Unit,
Addenbrooke's Hospital,
University of Cambridge,
P.O. Box 167, Cambridge, CB2 2QQ, UK
e-mail: sjp58@cam.ac.uk
Tel.: +44-1223-336933
Fax: +44-1223-216926

N. G. Burnet · R. Jena
Department of Oncology,
Addenbrooke's Hospital,
University of Cambridge,
Cambridge, CB2 2QQ, UK

Abstract The inherent invasiveness of malignant cells is a major determinant of the poor prognosis of cerebral gliomas. Diffusion tensor MRI (DTI) can identify white matter abnormalities in gliomas that are not seen on conventional imaging. By breaking down DTI into its isotropic (p) and anisotropic (q) components, we can determine tissue diffusion “signatures”. In this study we have characterised these abnormalities in peritumoural white matter tracts. Thirty-five patients with cerebral gliomas and seven normal volunteers were imaged with DTI and T2-weighted sequences at 3 T. Displaced, infiltrated and disrupted white matter tracts were identified using fractional anisotropy (FA) maps and directionally encoded colour maps and characterised using tissue signatures. The diffusion tissue signatures were normal in ROIs where the white matter was displaced. Infiltrated white matter was characterised by an increase in the isotropic component of the tensor (p) and a less marked reduction of the anisotropic component

(q). In disrupted white matter tracts, there was a marked reduction in q and increase in p . The direction of water diffusion was grossly abnormal in these cases. Diffusion tissue signatures may be a useful method of assessing occult white matter infiltration.

Keywords Magnetic resonance · Diffusion tensor · Neoplasms · Brain · White matter

Introduction

The diffuse infiltration of white matter tracts by cerebral gliomas is a major cause of their appalling prognosis. Tumour cells invade white matter tracts and can later destroy them [1]. In addition, the tumour mass can displace these white matter tracts [2]. It is well appreciated that glioma cells can spread beyond the abnormal area seen

on conventional MRI [3–5]. An ability to identify and characterise white matter involvement should allow better planning of current glioma therapies and may be a useful tool to monitor the response to therapy.

Diffusion tensor imaging (DTI) is a technique that is sensitive to the ordered anisotropic diffusion of water along white matter tracts. It can identify subtle white matter abnormalities in a number of disorders [6–9]. We

have previously shown that DTI can identify larger areas of signal abnormality in patients with high grade gliomas when compared with conventional T_2 -weighted sequences [10]. Most attempts to quantify the information in the diffusion tensor have determined the relative magnitudes of diffusion along three orthotropic directions (the eigenvalues). The direction (or eigenvector) of the largest eigenvalue indicates the principal axis of diffusion and can identify the direction of the white matter tracts. The eigenvalues can be used to calculate various indices of diffusion. Most published studies, however, only use two measures, fractional anisotropy (FA) as a measure of anisotropic diffusion and the mean diffusivity (D) as a measure of isotropic diffusion. Basser pointed out, however, that it is likely different indices of diffusion will identify different pathological and physiological characteristics of the tissue studied [11]. Green et al. have shown that FA may be insensitive to the changes seen in acute stroke [12]. They suggested a method that decomposes the tensor into its isotropic component (p) and its anisotropic component (q) using standardised engineering models. The p and q values can be plotted as the x and y axes of a graph (referred to as the pq plane) to simultaneously display the isotropic and anisotropic values from a defined region of interest (ROI). Different tissues have different values of p and q so will have different locations in the pq plane. These different locations can be referred to as diffusion tissue signatures.

In this study, we have used these diffusion tissue signatures in 35 patients with cerebral gliomas to understand the pathological changes that occur in the peritumoural brain. We have attempted to characterise these changes in terms of the interactions of the tumour with white matter tracts. In addition, we have attempted to define what biological characteristics of the tissue these pq -values represent.

Methods

Patients

Thirty-five patients with cerebral gliomas (mean age 44.7 years, range 25–80) and seven normal volunteers (mean age 31.6 years, range 24–54) were prospectively recruited for this study. The histology of the gliomas was 11 WHO Grade IV glioblastomas, 7 WHO Grade III gliomas and 17 WHO Grade II low grade gliomas. All studies were approved by the Cambridge Local Research Ethics Committee, and written, informed consent was obtained from all patients.

Imaging sequences and analysis

Imaging was performed at 3 T (Bruker, Etlingen, Germany). All patients were imaged in the axial plane with 4-mm slice thickness and using a 1-mm interslice separation. Imaging consisted of T_2 /proton density fast spin echo sequence (TR=6,055 ms; TE=80 ms/20 ms; FOV=35.84×16.8 cm²; matrix 512×256; 27 slices), and a single-shot, spin echo, echo planar imaging (EPI)

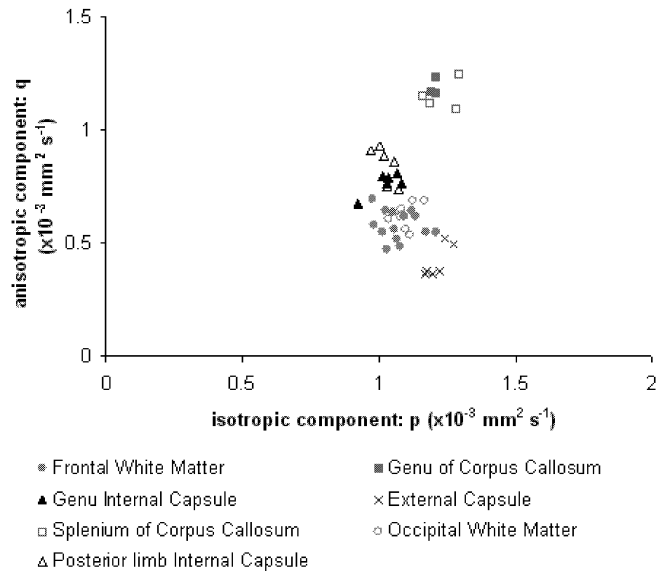


Fig. 1 Tissue signatures taken from ROI in a 24-year-old healthy male volunteer. Although values demonstrate a limited range of isotropic values (p), there is a marked range of q -values. Commissural fibres of the corpus callosum have a higher anisotropic value than the internal capsule, which in turn are higher than the frontal or occipital white matter. Values from the genu and splenium of the corpus callosum were similar, as were values from the genu and posterior limb of the internal capsule

diffusion tensor sequence (TR=5,070 ms; TE=107 ms; FOV=25×25 cm²; matrix 128×128; between 8 and 27 slices). Each slice from the DTI sequence was collected from 12 non-collinear gradient directions [13]. For each direction one T_2 (b_0) image and five diffusion gradient weighted images were collected (318, 392.5, 785, 1177.5 and 1,570 s/mm²) [13].

The diffusion tensor was calculated on a voxel-by-voxel basis as the solution of the Stejskal-Tanner equation with an in-house program implemented in MATLAB (The MathWorks, Inc., Natick, MA), following the method proposed by Basser [11, 14]. For each voxel the eigenvalues ($\lambda_1, \lambda_2, \lambda_3$) are computed, and then used to calculate fractional anisotropy as well as p and q using the following equations:

$$p = \sqrt{3}D \quad (1)$$

$$q = \sqrt{(\lambda_1 - D)^2 + (\lambda_2 - D)^2 + (\lambda_3 - D)^2} \quad (2)$$

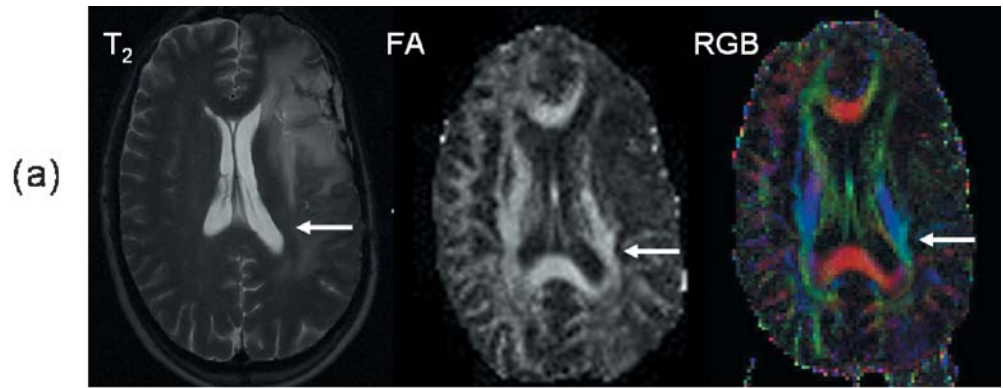
where D is the mean diffusivity:

$$D = (\lambda_1 + \lambda_2 + \lambda_3)/3 \quad (3)$$

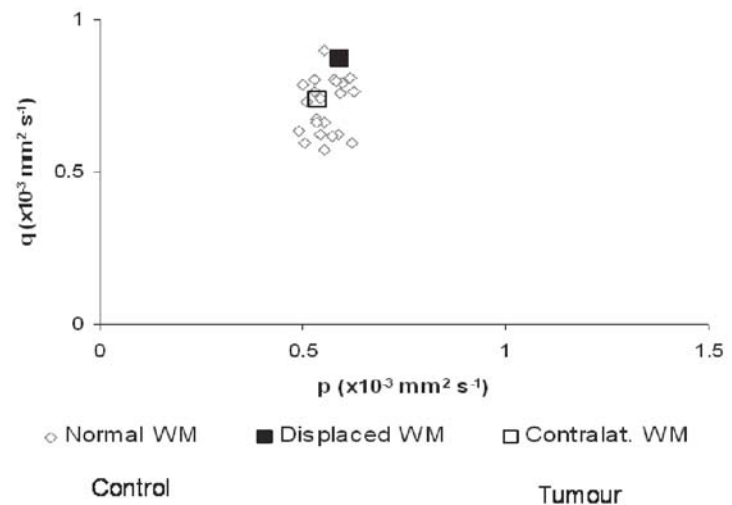
Directionally encoded colour maps were created using the method described by Pajevic [15] by colouring the components of the main eigenvector red, green and blue (RGB), respectively. Thus, the voxels with fibres lying in the x -direction (left-right) appear red; fibres lying in the y -direction (anterior-posterior) appear green, and those lying in the z -direction (superior-inferior) appear blue. In the resultant maps the intensity of each voxel is weighted by its fractional anisotropy. Therefore, voxels without a strong directionality appear black.

The spatial orientation of the main eigenvector was also investigated by plotting separately its coronal (coloured green) and axial projections (coloured blue). The resultant "rose plot" was then used to quantify the direction (in degrees) of the main eigenvector in each plane.

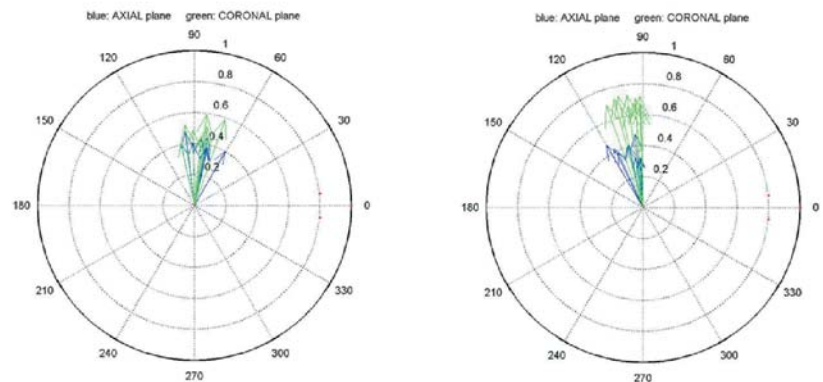
Fig. 2 An example from a 47-year-old man with a glioblastoma (WHO Grade IV) displacing white matter (*area arrowed in a*). **b** The tissue signature from this region was similar to one taken from the contralateral white matter. These values were similar to values from our normal volunteers. **c** Principal axis analysis shows that the spread and magnitude of the diffusion vectors are the same on the displaced side as they are on the contralateral side



(b)



(c)



Analysis of regions of interest

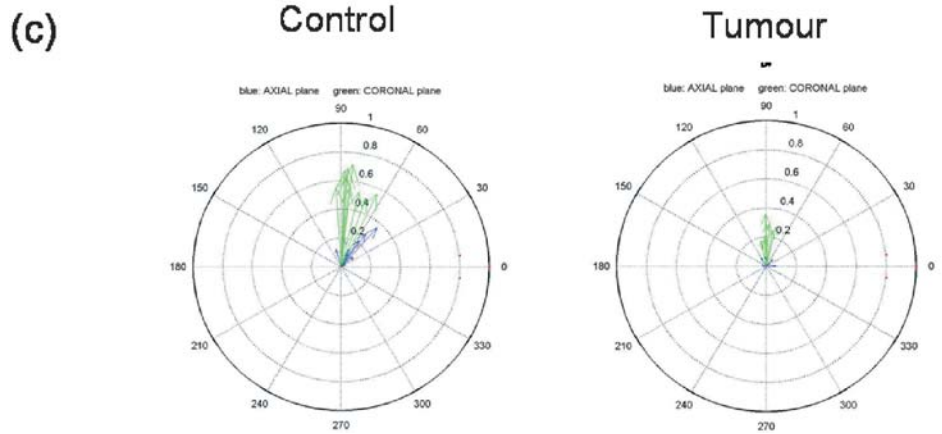
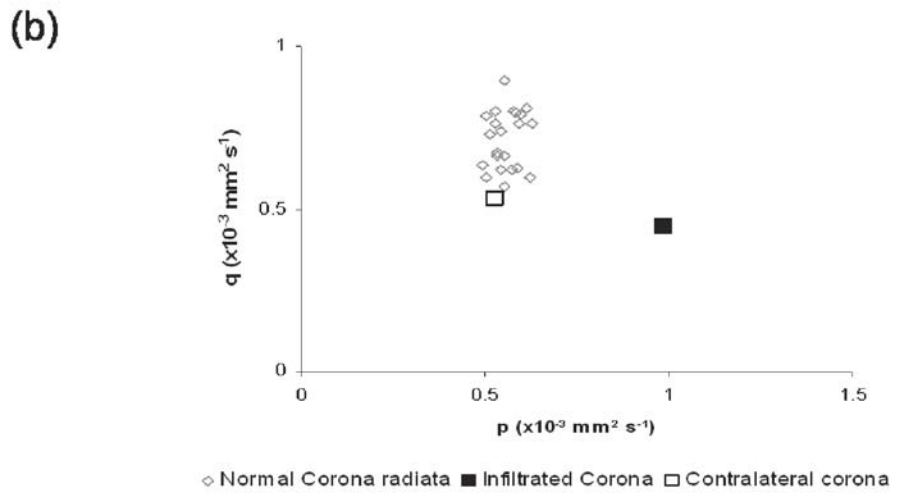
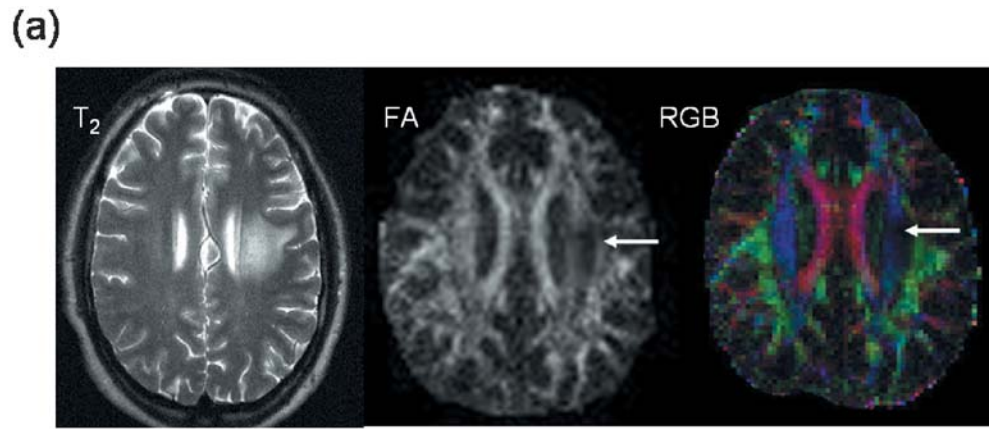
Using the FA maps from the normal volunteers, regions of interest (ROI) were selected from the following white matter tracts:

1. Frontal white matter
2. Genu of corpus callosum
3. Splenium of corpus callosum

4. Genu of internal capsule
5. Posterior limb of internal capsule
6. External capsule
7. Occipital white matter

For each of these regions both p and q were determined. Plots of normal tissue signatures were performed by plotting p on the x -axis and q on the y -axis of a graph (Fig. 1 is an example from a normal volunteer).

Fig. 3 An example of an infiltrated white matter tract (arrowed) in a 32-year-old man with a glioblastoma (WHO Grade IV). There is a reduction in the FA but the tract is still visible. **b** The tissue signatures show a large increase in p with only a small decrease in q . **c** The principal axis analysis shows no change in the spread of the diffusion vectors, but a marked reduction in the magnitude of the vectors



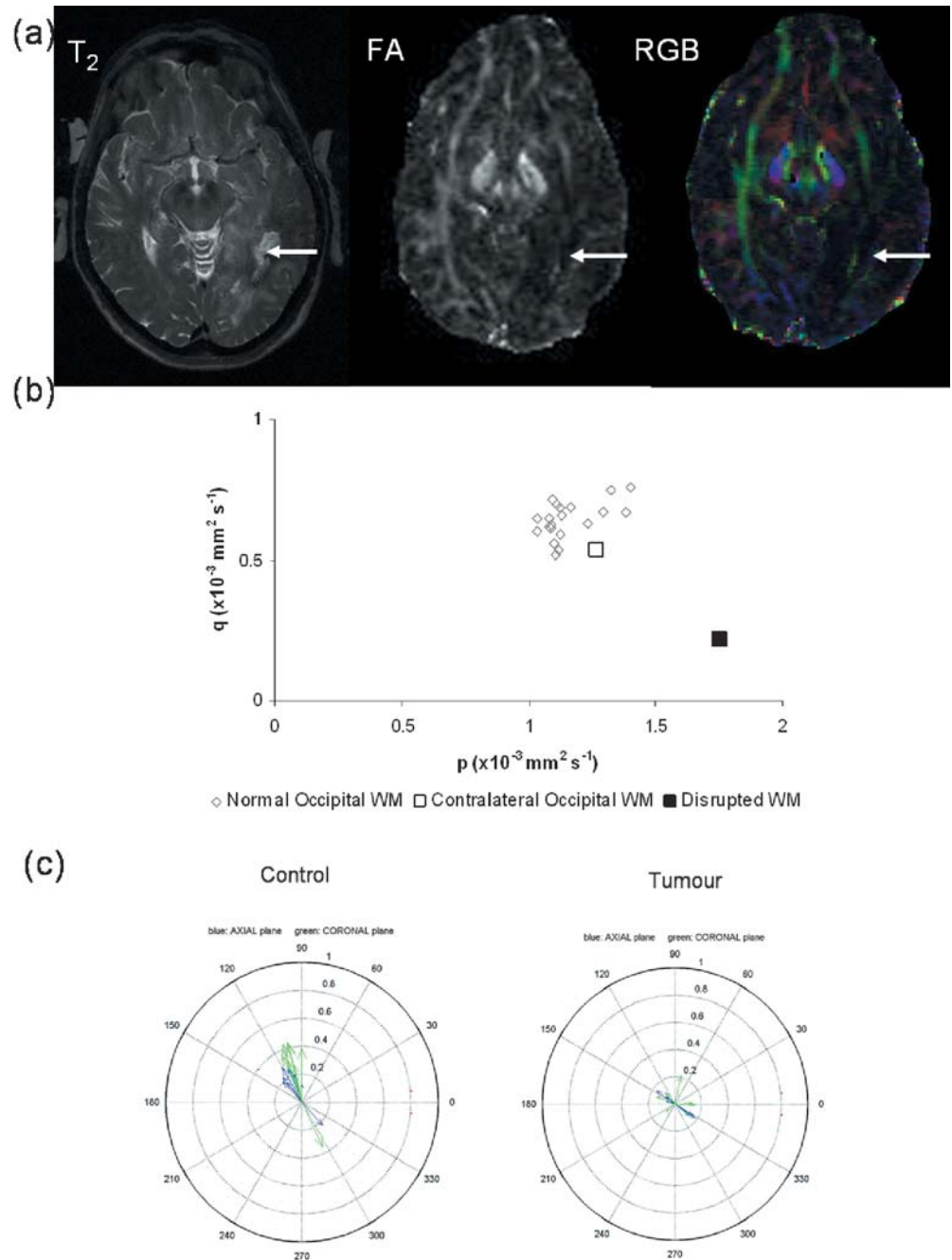
For the glioma patients ROIs were selected from the centre of the tumour and within the peritumoural white matter according to the classification described by Witwer [16] using FA maps and RGB colour orientation maps. Briefly, this separated ROI into three main types:

1. Displaced white matter tract: no change in FA compared to the normal contralateral side but alterations in fibre orientation on the RGB colour orientation maps (example shown in Fig. 2 a)

2. Infiltrated white matter tract had reduced FA, but the tract was still identifiable on the orientation maps (example shown in Fig. 3 a)
3. Disrupted tracts had reduced FA and could not be identified on orientation maps (example shown in Fig. 4 a)

For each ROI a control in the opposite hemisphere was also identified. Values of p and q were determined and tissue signatures plotted for every ROI. Rose diagrams for each region were plotted and mea-

Fig. 4 **a** An example of a disrupted occipital white matter in a 74-year-old woman with a glioblastoma (WHO Grade IV). The occipital white matter tract cannot be identified on the FA map. **b** In this region the tissue signatures show a marked increase in p and a marked decrease in q . **c** The principal axis analysis shows spread of the direction of the white matter tracts and marked reduction in the magnitude of the diffusion



tures of the length of the largest eigenvector (the magnitude of diffusion) and the spread of eigenvectors (directionality of diffusion) were derived. The data were analysed using SPSS for Windows (release 11.0.0, 2001). Significance was taken at the 0.05 level.

Results

Normal volunteers

The different white matter tracts could be identified in all the volunteers. Measurements of p and q are sum-

marised in the Table 1 and have been plotted for a single volunteer in Fig. 1. The isotropic component p varied little for different white matter ROI. Values were lowest in the internal capsule ($0.95 \pm 0.02 \times 10^{-3} \text{ mm}^2 \text{ s}^{-1}$), and highest in the corpus callosum ($1.24 \pm 0.07 \times 10^{-3} \text{ mm}^2 \text{ s}^{-1}$). The q -values were more varied and were highest in the commissural fibres of the corpus callosum ($1.07 \pm 0.05 \times 10^{-3} \text{ mm}^2 \text{ s}^{-1}$) and lowest in the association fibres of the frontal and occipital lobes as well as the external capsule (e.g., in the external capsule q was $0.43 \pm$

Fig. 5 Tissue signatures from the tumour in both low grade (WHO Grade II) and high grade (WHO Grades III and IV) gliomas. The p -values are significantly higher in the low grade tumours, possibly reflecting the increased cellularity and restriction of water diffusion in high grade gliomas. The q -values are not significantly different in the two tumour groups

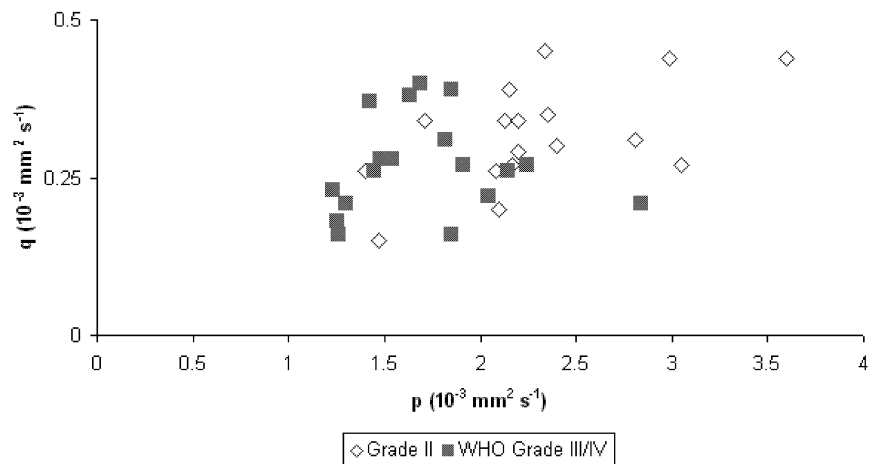


Table 1 pq -Values for white matter regions in normal volunteers

White matter region	Isotropic component (p) ($\times 10^{-3} \text{ mm}^2 \text{ s}^{-1}$)	Anisotropic component (q) ($\times 10^{-3} \text{ mm}^2 \text{ s}^{-1}$)
Genu of corpus callosum	1.23 \pm 0.1	1.05 \pm 0.12
Splenium of corpus callosum	1.24 \pm 0.09	1.07 \pm 0.07
Genu internal capsule	0.96 \pm 0.04	0.71 \pm 0.09
Posterior limb of internal capsule	0.95 \pm 0.03	0.81 \pm 0.05
Frontal white matter	1.09 \pm 0.07	0.51 \pm 0.08
Occipital white matter	1.16 \pm 0.11	0.64 \pm 0.06
External capsule	1.18 \pm 0.05	0.42 \pm 0.06

All figures are quoted as the mean \pm 95% CI.

$0.06 \times 10^{-3} \text{ mm}^2 \text{ s}^{-1}$). Tissue signatures from similar white matter tracts appeared in similar regions of the pq plot. For example, there were no differences in p and q from ROIs taken from either the genu or splenium of the corpus callosum, or from those taken from either the genu or posterior limb of the internal capsule.

Glioma patients

Diffusion tissue measurements from the normal brain in the glioma patients were essentially similar to the normal controls. For many patients the p -value was at the upper end and the q -value at the lower end of the normal range.

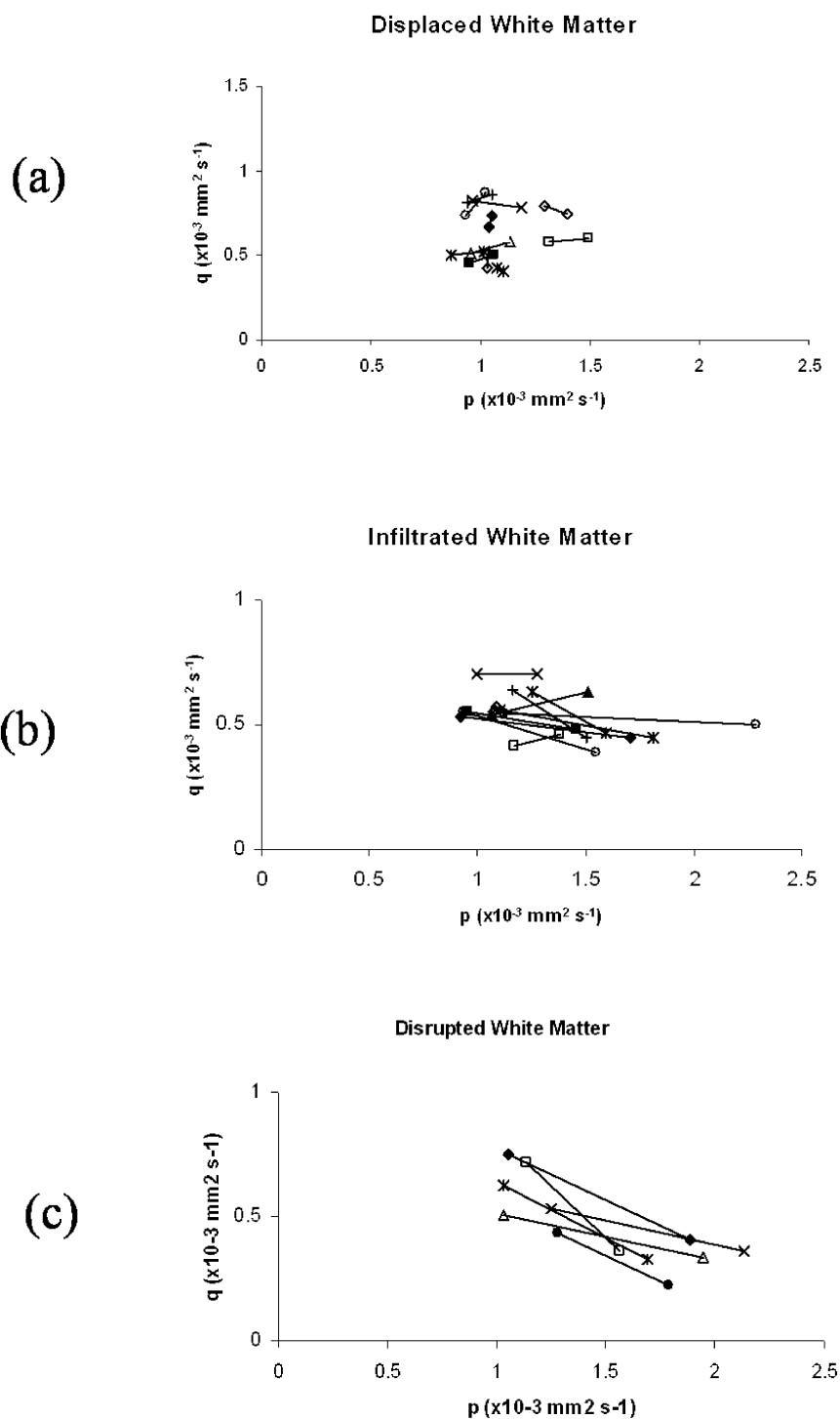
Measurements taken from the tumours differed with the different tumour grades (Fig. 5). The p -value for low grade gliomas (WHO Grade II) was significantly higher than in high grade tumours (WHO Grades III and IV) (mean value \pm 95% confidence interval Grade II is 2.3 ± 0.27 vs. 1.72 ± 0.1 for Grades III and IV; $p=0.01$). The q -value in the low grade tumours is slightly higher than in high grade tumours, although this is not significantly different (0.32 ± 0.02 vs 0.27 ± 0.02 ; $p=0.08$). In the low grade gliomas, there was evidence of white matter disruption within the tumour, but none in the surrounding peritumoural white matter. Extensive disruption was seen in the WHO Grade IV tumours.

Measurements taken in the white matter tracts that were considered to be displaced showed little difference in either of these components. The value of p from displaced white matter did not differ from measurements taken from the contralateral, normal white matter tract (mean ratio \pm 95% confidence interval of normal to abnormal p -value is 1.03 ± 0.07). The q -value was also similar to the contralateral tract (ratio 1.08 ± 0.05) (Fig. 6 a, plus an example of a patient is seen in Fig. 2). For infiltrated white matter tracts, the p -values had a mean increase of 50% (95% CI \pm 20%) compared to contralateral, normal white matter. There was a slight decrease in q -value in the infiltrated tracts ($14 \pm 9\%$) (Fig. 6 b, plus an example of a patient is seen in Fig. 3). The disrupted tracts, however, showed a marked increase in p ($68 \pm 17\%$) and a marked decrease in q (mean decrease of $42 \pm 7\%$) (Fig. 6 c, plus an example of a patient is seen in Fig. 4).

Principal axis of diffusion analysis in glioma patients

The magnitude and spread of the principal axis of diffusion could be determined in all ROI. In the displaced tracts neither the magnitude of diffusion (0.66 ± 0.1 vs. 0.7 ± 0.1 for controls; $p=0.43$) nor the spread of the principal axes was altered compared to the non-tumour side ($29.4^\circ \pm 8.4$ vs. $26.9^\circ \pm 4.8$ for controls; $p=0.62$) (Fig. 2 c).

Fig. 6 Tissue signatures from regions of white matter that are **a** displaced, **b** infiltrated by tumour and **c** disrupted. All values are compared to the similar tracts in the contralateral hemisphere. Tissue signatures in displaced white matter tracts are similar to contralateral white matter. In the infiltrated white matter the main change is the increase in p . In disrupted white matter tracts there is a marked increase in p and reduction in q



For infiltrated white matter tracts the magnitude of diffusion decreased (0.44 ± 1.0 vs. 0.69 ± 0.6 for control; $p=0.001$), but the spread of the principal axis was unchanged ($28.3^\circ \pm 7.1$ vs. $24.2^\circ \pm 5.0$ for controls; $p=0.37$) (Fig. 3 c). In disrupted white matter tracts there was

a marked decrease in the magnitude of diffusion (0.27 ± 0.06 vs. 0.64 ± 0.12 for controls; $p=0.0003$) with a corresponding increase in the spread of principal axes of diffusion ($75.5^\circ \pm 33.4$ vs. $31.2^\circ \pm 11.6$ for controls; $p=0.03$) (Fig. 4 c).

Discussion

In this study we have shown that by decomposing the diffusion tensor into isotropic (p) and anisotropic (q) components we can plot this information as a diffusion tissue signature. These tissue signatures are different for different white matter tracts and are unaffected by displacement of white matter tracts by tumours. Tumour infiltration of white matter fibres causes an increase in the isotropic component (p), whereas a reduction in the anisotropic component occurs with disruption of white matter fibres (q).

Our finding of different white matter tracts having different tissue signatures relates to the variation in the anisotropic properties of various tracts. We have shown that commissural fibres have greater anisotropy compared to projection fibres, which in turn have greater anisotropy compared to association fibres. These findings are mirrored by other studies [17–20]. Chepuri postulated that these differences could be due to either (1) tighter packing of fibres, (2) less permeable myelin sheaths or (3) altered radius of individual axons [19]. They were, however, unable to demonstrate these differences with their limited post-mortem material. Pierpaoli [17] suggested that there were no specific structural features that could account for these changes. They showed that although the anisotropic index of the pyramidal tracts were similar to the corpus callosum, the fibre density of the latter was almost five times greater. They also pointed out that the thickness of myelin is relatively uniform over the brain and that white matter fascicles contain axons of variable diameter.

It is interesting to note that our pq -values from the normal white matter of our tumour patients were often just outside the ranges from our normal volunteers. Frequently the p -value was fractionally higher and the q lower than these volunteers. The reason for this relates to the differences in age between the two groups (mean age of tumour patients 44.7 years, mean age of volunteers 31.6 years). Increased age appears to increase the isotropic diffusion component and decrease the anisotropic index [21, 22]. To be certain that tissue signatures were significantly different from normal, it was essential to refer to age-matched values. As our data from our normal volunteers are not age-matched, it can only be used as a guide to where the normal range would be expected.

Using the techniques described by Witwer [16], we have been able to develop a better understanding of the changes that occur during tumour invasion. Although we have not obtained histological evidence of tumour infiltration in this study, Witwer confirmed their findings by taking image-guided biopsies at the time of tumour resection. We found that when a white matter tract is displaced by the tumour mass, there are no changes in either the isotropic or anisotropic components of the tensor. Analysis of the principal axis of diffusion shows

this is distorted, but has no difference in either the spread or magnitude of the diffusion vector. Careful histological studies by Scherer in the 1930s have shown that initial tumour growth frequently involves the formation of “secondary structures” where glioma cells grow between and around neurons and extend into white matter tracts [1]. At this stage of tumour invasion, there is an increase in cellularity without disruption of neurons, and this would correspond to our findings of an increase in isotropic diffusion with minimal change in anisotropy. Later tumour growth replaces neurons in what Scherer referred to as neurophagic growth. We have found that this stage corresponds with a marked increase in isotropic diffusion and a reduction in anisotropic diffusion.

It is easy to understand why the destruction of neurons can lead to the decrease in anisotropy (i.e., reduction of q); changes in isotropic diffusion indices are less straightforward. Sinha has shown that within tumours there is an increase in mean diffusivity D (which is closely related to p , see Eqs. 1, 3) [23]. They suggested this is due to an increased amount of water in the tissue due to vasogenic oedema. Lu also found an increase in D in the peritumoural brain of both metastases and high grade gliomas [24]. They also found that the increase in D was greater for metastases than gliomas, a finding probably related to the marked oedema frequently seen with even small metastases [25]. It seems likely that p does relate to the oedema in these regions. If it was due to changes in cellularity, a reduction in water mobility would be expected, and hence a decrease in the mean diffusivity. Sinha showed that in the enhancing rim of a high grade glioma, an area with marked increase in cellularity, there is a decrease in mean diffusivity. This may explain why we saw a decrease in p in higher grade tumours with increased tumour cellularity. Interestingly, the findings of decreased magnitude of water diffusion vectors seen with our principal axis analysis with increase in p -value could be explained by a reduction in water mobility due to increased tumour cellularity.

Tissue signature analysis of tumour involvement of white matter tracts appears to have advantages over using FA. As Green et al. showed, FA is a ratio of the anisotropic component of the diffusion tensor (q) and the Euclidean length of the tensor (L) [12]. As a result, FA can change due to alterations in either q or L . The relationship between pathological changes within the tumour and FA is a complex one. Beppu [20] found that FA correlated with tumour cellularity, but FA in the tumour was lower than in normal white matter. They suggested the FA value is in fact a balance between reduced FA due to loss of directionality of diffusion from fibre disruption and the increase due to cellularity. Their four patients with gliomatosis cerebri, a condition characterised by growth of parallel rows of tumour cells along neurons without destroying them [26], had increased FA, reflecting increased tumour cellularity.

Conclusion

Tissue signatures appear to demonstrate different aspects of tumour behaviour. The isotropic p component appears to increase with tumour infiltration due to the increased tissue water from vasogenic oedema. Analysis of the principal axis shows reduction of the vector magnitude probably relating to the reduced water mobility caused by increased tumour cellularity. Reduction of the anisotropic component q occurs when there is disruption of white

matter tracts. The information this technique provides is important in planning the treatment of gliomas and, since several of the changes seen here relate to tumour cell infiltration and cellularity, it is likely DTI could provide a useful method of assessing response to therapy.

Acknowledgements The study was funded by the New and Emerging Applications of Technology (NEAT) Programme from the Department of Health and in part by a Technology Foresight Award. We wish to thank Ruth Bisbrown-Chippendale, Claire Sleator and Victoria Lupson for their assistance.

References

- Scherer HJ (1938) Structural development in gliomas. *Am J Cancer* 34:333–351
- Wieshmann UC, Symms MR, Parker GJ, Clark CA, Lemieux L, Barker GJ, Shorvon SD (2000) Diffusion tensor imaging demonstrates deviation of fibres in normal appearing white matter adjacent to a brain tumour. *J Neurol Neurosurg Psychiatry* 68:501–503
- Hawighorst H, Schreiber W, Knopp MV, Essig M, Engenhart CR, Brix G, van Kaick G (1996) Macroscopic tumor volume of malignant glioma determined by contrast-enhanced magnetic resonance imaging with and without magnetization transfer contrast. *Magn Reson Imaging* 14:1119–1126
- Johnson PC, Hunt SJ, Drayer BP (1989) Human cerebral gliomas: correlation of postmortem MR imaging and neuropathologic findings. *Radiology* 170:211–217
- Watanabe M, Tanaka R, Takeda N (1992) Magnetic resonance imaging and histopathology of cerebral gliomas. *Neuroradiology* 34:463–469
- Ulug AM, Moore DF, Bojko AS, Zimmerman RD (1999) Clinical use of diffusion-tensor imaging for diseases causing neuronal and axonal damage. *AJNR Am J Neuroradiol* 20:1044–1048
- Filippi CG, Ulu AM, Ryan E, Ferrando SJ, van Gorp WW (2001) Diffusion tensor imaging of patients with HIV and normal-appearing white matter on MR images of the brain. *AJNR Am J Neuroradiol* 22:277–283
- Wieshmann UC, Clark CA, Symms MR, Franconi F, Barker GJ, Shorvon SD (1999) Reduced anisotropy of water diffusion in structural cerebral abnormalities demonstrated with diffusion tensor imaging. *Magn Reson Imaging* 17:1269–1274
- Huisman TA (2003) Diffusion-weighted imaging: basic concepts and application in cerebral stroke and head trauma. *Eur Radiol* 13:2283–2297
- Price SJ, Burnet NG, Donovan T, Green HA, Pena A, Antoun NM, Pickard JD, Carpenter TA, Gillard JH (2003) Diffusion tensor imaging of brain tumours at 3 T: a potential tool for assessing white matter tract invasion? *Clin Radiol* 58:455–462
- Basser PJ, Pierpaoli C (1996) Microstructural and physiological features of tissues elucidated by quantitative-diffusion-tensor MRI. *J Magn Reson B* 111:209–219
- Green HA, Pena A, Price CJ, Warburton EA, Pickard JD, Carpenter TA, Gillard JH (2002) Increased anisotropy in acute stroke: a possible explanation. *Stroke* 33:1517–1521
- Papadakis NG, Xing D, Haung LH, Hall LD, Carpenter TA (1999) A comparative study of acquisition schemes for diffusion tensor imaging using MRI. *J Magn Reson B* 137:67–82
- Basser PJ, Mattiello J, LeBihan D (1994) Estimation of the effective self-diffusion tensor from the NMR spin echo. *J Magn Reson B* 103:247–254
- Pajevic S, Pierpaoli C (1999) Color schemes to represent the orientation of anisotropic tissues from diffusion tensor data: application to white matter fiber tract mapping in the human brain. *Magn Reson Med* 42:526–540
- Witwer BP, Moftakhar R, Hasan KM, Deshmukh P, Haughton V, Field A, Arfanakis K, Noyes J, Moritz CH, Meyerand ME, Rowley HA, Alexander AL, Badie B (2002) Diffusion-tensor imaging of white matter tracts in patients with cerebral neoplasm. *J Neurosurg* 97:568–575
- Pierpaoli C, Jezzard P, Basser PJ, Barnett A, Di Chiro G (1996) Diffusion tensor MR imaging of the human brain. *Radiology* 201:637–648
- Shimony JS, McKinstry RC, Akbudak E, Aronovitz JA, Snyder AZ, Lori NF, Cull TS, Conturo TE (1999) Quantitative diffusion-tensor anisotropy brain MR imaging: normative human data and anatomic analysis. *Radiology* 212:770–784
- Chepuri NB, Yen YF, Burdette JH, Li H, Moody DM, Maldjian JA (2002) Diffusion anisotropy in the corpus callosum. *AJNR Am J Neuroradiol* 23:803–808
- Beppu T, Inoue T, Shibata Y, Kurose A, Arai H, Ogasawara K, Ogawa A, Nakamura S, Kabasawa H (2003) Measurement of fractional anisotropy using diffusion tensor MRI in supratentorial astrocytic tumours. *J Neurooncol* 63:109–116
- Abe O, Aoki S, Hayashi N, Yamada H, Kunitatsu A, Mori H, Yoshikawa T, Okubo T, Ohtomo K (2002) Normal aging in the central nervous system: quantitative MR diffusion-tensor analysis. *Neurobiol Aging* 23:433–441
- O'Sullivan M, Jones DK, Summers PE, Morris RG, Williams SC, Markus HS (2001) Evidence for cortical “disconnection” as a mechanism of age-related cognitive decline. *Neurology* 57:632–638
- Sinha S, Bastin ME, Whittle IR, Wardlaw JM (2002) Diffusion tensor MR imaging of high-grade cerebral gliomas. *AJNR Am J Neuroradiol* 23:520–527
- Lu S, Ahn D, Johnson G, Cha S (2003) Peritumoral diffusion tensor imaging of high-grade gliomas and metastatic brain tumors. *AJNR Am J Neuroradiol* 24:937–941
- Kleihues P, Cavenee WK (2000) Pathology and genetics of tumours of the nervous system. IARC, Lyon
- Artigas J, Cervos-Navarro J, Iglesias JR, Ebhardt G (1985) Gliomatosis cerebri: clinical and histological findings. *Clin Neuropathol* 4:135–148